ISSN 1061-933X, Colloid Journal, 2013, Vol. 75, No. 2, pp. 150–158. © Pleiades Publishing, Ltd., 2013.
Original Russian Text © A.E. Galashev, 2013, published in Kolloidnyi Zhurnal, 2013, Vol. 75, No. 2, pp. 170–178.

Adsorption of Ammonia by Water Clusters. Computer Experiment

A. E. Galashev

Institute of Industrial Ecology, Ural Branch, Russian Academy of Sciences, ul. Sof'i Kovalevskoi 20, Yekaterinburg, 620990 Russia

Received May 3, 2012

Abstract—The method of molecular dynamics is used to study the adsorption of from one to six ammonia molecules by water clusters composed of 50 molecules. The adsorption of NH_3 molecules markedly increases the IR absorption spectrum intensity, substantially decreases emission power in the frequency range of $0 \leq \omega \leq 3500$ cm^{-1}, and transforms a continuous reflectance spectrum into a banded one. A rough surface formed by adsorbed ammonia molecules reduces the absorption coefficient and refractive index of the system of water–ammonia clusters in the entire frequency range. Adsorption of ammonia molecules by water clusters greatly diminishes the number of electrons that are active with respect to electromagnetic radiation.

DOI: 10.1134/S1061933X13020063

INTRODUCTION

Many experimental [1–5] and theoretical [6–13] works have been devoted to studying the structure, thermodynamic properties, and spectra of small water clusters, because they play important roles in various phenomena, including ion solvation, as well as the processes of dissolution in biological and chemical systems [14, 15]. $NH_3(H_2O)$ complexes have been experimentally studied with the help of the methods of microwave and IR spectroscopy [16], as well as ab initio calculations [17]. The structure and thermodynamic and kinetic properties of $NH_3(H_2O)_n$, complexes, where $n = 1$ and 2, have been investigated in [18]. The data obtained in [19] suggest that at least four water molecules must be present in a cluster to provide its dissociation yielding NH_4^+ and OH^- ions. The dissociation is determined by proton transfer from one water molecule to an ammonium molecule. Theoretical information that includes data on the structure and dissociation energy of $NH_4^+\cdots(H_2O)_n\cdots OH^-$, systems, where $n = 5$, 8, 9, and 21, has been obtained in [20]. The free energy increments resulting from dissociation diminish with an increase in the number of water molecules in the clusters. As the number of water molecules in both dissociated and nondissociated aggregates increases, the frequencies of the stretching vibrations of NH and OH bonds decrease. The frequencies of OH modes in ion-containing clusters are lower than those in ion-free clusters. As soon as an ion pair is formed in a cluster, its NH mode exhibits a red shift.

Ammonia has a noticeable effect on atmospheric processes because of its high valence, which determines its role as a potential site of proton sink and ionic nucleation. The combined action of ammonia and sulfuric acid enhances atmospheric nucleation. Ammonia plays an important role in the chemistry of the cloud layers of Jupiter and Saturn, and a substantial amount of ammonia has been found on Uranus and Neptune [21]. The interaction of ammonia with water yields ammonium hydroxides. Under normal conditions, saturated ammonia solutions are characterized by an NH_3-to-H_2O ratio of 1 : 1, mol/mol. Strong cooling of such a solution (to ≈190 K) gives rise to crystallization of ammonia hydrate $NH_3 \cdot H_2O$. Hydrate of the $NH_3 \cdot 2H_2O$ composition (dihydrate) is known to prevail at low pressures. In addition to phase I of ammonium dihydrate, which is observed at common low pressures, three high-pressure phases (II–IV) have been found [22]. At a pressure of ≈3.5 GPa, ammonia dihydrate is instable and can form a mixture of high-pressure ammonia hydrate and water ice [22]. Weak hydrogen bonding between adjacent ammonia molecules results in its pseudodense packing in the solid state [23]. The weak hydrogen bonding and the formation of homo- and heteronuclear hydrogen bonds determine the need for application of the methods that are used to study the electron structure [24]. In this case, the main difficulty is to energetically describe the proton transfer because of the high transferred charge. Moreover, electron correlation results in exchange interactions involving van der Waals forces.

At present, mathematical simulation is the main source of information on the infrared band intensities of the clusters. Direct measurement of this characteristic is, in most cases, complicated by the difficulties connected to determination of the absolute number density. The strong enhancement of the infrared band intensities of different hydrogen-bonded clusters suspended in a cryogenic matrix was discovered several dozen years ago [25]. However, the spectrum broadening and the complex kinetic of cluster formation in

solid matrices made it impossible to determine this characteristic for clusters of a certain size. This problem was solved using the technique of encapsulation into helium droplets [26]. The quantum nature of helium droplets at very low temperatures enabled researchers to form molecular clusters and avoid spectral broadening.

The goal of this work was to study the optical effects resulting from adsorption of ammonia molecules by large water clusters (these effects manifesting themselves as changes in the spectra of IR absorption, emission, and reflection) and determine the frequency dependences of characteristics of geometrical optics, i.e., the absorption coefficients and refractive indices of water–ammonia disperse systems.

MOLECULAR-DYNAMIC MODEL

The interaction of water molecules in clusters is described by a nonadditive potential, the additive component of which is represented by the modified [27] TIP4P potential for water [28], while its nonadditive component is determined by the polarization interaction; thus, the potential energy of the system is described in the following manner:

$$U_{\text{tot}} = U_{\text{pair}} + U_{\text{pol}},$$

where the pair component of the potential energy is determined by the Lennard-Jones and Coulomb contributions as follows:

$$U_{\text{pair}} = \sum_i \sum_j \left\{ 4\varepsilon^{(\text{LJ})} \left[\left(\frac{\sigma^{(\text{LJ})}}{r_{ij}} \right)^{12} - \left(\frac{\sigma^{(\text{LJ})}}{r_{ij}} \right)^{6} \right] + \frac{q_i q_j}{r_{ij}} \right\}.$$

Here, r_{ij} is the distance between atoms i and j, q is the electric charge, and $\sigma^{(\text{LJ})}$ and $\varepsilon^{(\text{LJ})}$ are the Lennard-Jones potential parameters [27].

Polarization energy is determined in the following way:

$$U_{\text{pol}} = -\frac{1}{2} \sum_i \mathbf{d}_i \cdot \mathbf{E}_i^0,$$

where $\mathbf{E}_i^0$ is the electric field strength generated by a system of fixed charges at a point of molecule i localization,

$$\mathbf{E}_i^0 = \sum_{j \neq i} \frac{q_j \mathbf{r}_{ij}}{r_{ij}^3},$$

and $\mathbf{d}_i$ is the induced dipole moment attributed to this molecule,

$$\mathbf{d}_i = \alpha_i^p \mathbf{E}_i,$$

where

$$\mathbf{E}_i = \mathbf{E}_i^0 + \sum_{j \neq i} \hat{\mathbf{T}}_{ij} \cdot \mathbf{d}_j.$$

Here, $\mathbf{E}_i$ is the total electric field strength at the point that determines molecule i in the polarization interaction; α_i^p is the polarizability of the molecule; $\hat{\mathbf{T}}_{ij}$ is the dipole–dipole interaction tensor,

$$\hat{\mathbf{T}}_{ij} = \frac{1}{|r_{ij}|^3} (3\mathbf{u}_{ij} \cdot \mathbf{u}_{ij} - \hat{1}),$$

where $\mathbf{u}_{ij}$ is the unit vector oriented in the direction of the $\mathbf{r}_i - \mathbf{r}_j$, vector; $\mathbf{r}_j$ and $\mathbf{r}_i$ are the vectors that determine the locations of polarization-active points i and j in the corresponding molecules, respectively; and $\hat{1}$ is the unit tensor of the 3×3 dimensionality.

According to [27], we assume that the magnitude of the permanent dipole moment for water molecule is equal to its experimental value of 1.848 D. The geometry of the H_2O molecule corresponds to the following experimental parameters of a molecule occurring in a gas phase: $r_{\text{OH}} = 0.09572$ nm and H–O–H angle of 104.5° [29]. Fixed charges ($q_{\text{H}} = 0.519e$, $q_M = -1.038e$) are attributed to atoms H and point M that lies in the bisector of the H–O–H angle at a distance of 0.0215 nm from the oxygen atom. The values of the charges and the position of point M have been selected so as to reproduce the experimental values of the dipole and quadrupole moments [30, 31], as well as the ab initio calculated energy of the dimer and the characteristic distances in it [32]. Stabilization of the short-range order in water clusters is, to a high extent, achieved due to the short-range Lennard-Jones potential, with the interaction center being attributed to the oxygen atom. In addition to the electric charge, the polarizability, which is necessary for describing the nonadditive polarization energy, is attributed to point M. Induced dipole moments $\mathbf{d}_i$ are calculated using the standard iteration procedure [27] at each time step. The accuracy of $\mathbf{d}_i$ determination is preset in the range of 10^{-5}–10^{-4} D.

The ammonia–ammonia interatomic interactions are determined by the Lennard-Jones and Coulomb contributions as follows:

$$\Phi_{\text{a-w}}(r) = \varepsilon_{\text{a-w}} \left[\left(\frac{r_0}{r_{ij}} \right)^{12} - 2 \left(\frac{r_0}{r_{ij}} \right)^{6} \right] + \frac{q_i q_j}{r_{ij}}.$$

The magnitudes of parameters $\varepsilon_{\text{a-w}}$, r_0, and q_i of H and N atoms in the NH_3, molecule were taken equal to 0.038 kcal/mol, 0.28525 nm, and 0.333e and 0.41314 kcal/mol, 0.38171 nm, and –0.999e, respectively [33]. The parameters of the Lennard-Jones potential that describes the ammonia–water interaction were found by the Berthelot–Lorentz formulas

$$\varepsilon_{\text{aw}}^{(\text{LJ})} = \sqrt{\varepsilon_{\text{a}}^{(\text{LJ})} \varepsilon_{\text{w}}^{(\text{LJ})}}, \quad \sigma_{\text{aw}}^{(\text{LJ})} = \frac{\sigma_{\text{a}}^{(\text{LJ})} + \sigma_{\text{w}}^{(\text{LJ})}}{2},$$

where $\varepsilon_a^{(LJ)}$, and $\varepsilon_w^{(LJ)}$ are the energy and $\sigma_a^{(LJ)}$, and $\sigma_w^{(LJ)}$ are the geometric parameters of the potential for N and H atoms of the ammonia molecule and O atom of the water molecule, respectively.

The ammonia molecule has the shape of a triangular pyramid, with a nitrogen atom occurring in the vertex. The base of the pyramid represents an equilateral triangle formed by H atoms. The H–N–H bond angle is 107°, which is close to the tetrahedral angle of 109°. The interatomic distances in the NH_3: molecule are $r_{NH} = 0.102$ nm and $r_{HH} = 0.164$ nm. The NH_3 molecule has a higher polarizability α^p (2.145 Å^3) and lower dipole moment d (1.47 D) than does the water molecule (1.49 Å^3 and 1.848 D, respectively) [34].

The trajectories of the centers of masses of molecules were determined by the fourth-order Gear method [35]. Time step Δt of integration was 0.2×10^{-16} s. In a molecular-kinetic calculation $4 \times 10^6 \Delta t$ long, the equilibration was preliminarily performed at $T = 233$ K for pure water clusters free of impurity molecules. The $(H_2O)_n$, cluster configuration corresponding to the time moment of 40 ps was further used as the initial configuration for simulating $(NH_3)_i(H_2O)_{50}$, heteroclusters with $1 \le i \le 6$. Each added NH_3 molecule was initially placed into a position such that the shortest distance between the atoms of this molecule and atoms of water molecules was about 0.6 nm. At the beginning, the centers of masses of NH_3 molecules were placed in the coordinate axes outside the water cluster. The initial orientation of ammonia molecules was arbitrary. A newly formed cluster was equilibrated within a time interval of $1.2 \times 10^6 \Delta t$ at $T = 233$ K; then, the desired physicochemical properties were calculated at the same temperature for $5 \times 10^6 \Delta t$. A system of $(NH_3)_i(H_2O)_{50}$ clusters was formed in accordance with cluster statistical weights, which were determined as follows. Let us consider the case of unpolarized light scattering when free path l of molecules is much shorter than light wavelength λ. Extinction (attenuation) ratio h of an incident beam is determined by, on the one hand, the Rayleigh formula [36] and, on the other hand, scattering coefficient ρ ($h = \frac{16\pi}{3}\rho$) [37] under an approximation of the scattering angle of 90°. Taking into account that $h = \alpha + \rho$, where α is the absorption coefficient, we have

$$N = \frac{2\omega^4}{3\pi c^4}\frac{(\sqrt{\varepsilon}-1)^2}{\alpha}\left(1-\frac{3}{16\pi}\right),$$

where N is the number of scattering centers per cubic centimeter. Here, c is the speed of light, ε is the medium dielectric permittivity, and ω is the incident wave frequency.

Let us form systems II and III from $(H_2O)_n$ and $(NH_3)_i(H_2O)_{50}$ clusters, respectively, in a manner such that a cluster containing i impurity molecules and n water molecules has the following statistical weight:

$$W_{in} = \frac{N_{in}}{N_\Sigma}, \quad 1 \le i \le 6, \quad 10 \le n \le 50 \ (\Delta n = 5),$$

where N_{in} is the number of clusters containing number n of water molecules and number i of NH_3 molecules per cubic centimeter, $N_{1\Sigma} = \sum_{n=1}^{9} N_{i=0,n}$, $N_{2\Sigma} = \sum_{i=1}^{6} N_{i,n=50}$. Then, all spectral characteristics were calculated with allowance for the accepted statistical weights W_{in}..

The equations of motion for molecule rotation were analytically solved using the Rodrigo–Hamilton parameters [38], while the equations of motion involving rotations were integrated according to the Sonnenschein approach [39].

DIELECTRIC PROPERTIES

Total dipole moment $\mathbf{d}_{cl}$ of a cluster was calculated by the following formula:

$$\mathbf{d}_{cl}(t) = Z_+ \sum_{i=1}^{N_{tot1}} \mathbf{r}_i(t) + Z_- \sum_{j=1}^{N_{tot2}} \mathbf{r}_j(t),$$

where $\mathbf{r}_i(t)$ is the vector indicating the location of atom i or point M at time moment t; Z is the electric charge located in the center under consideration; subscript "+" refers to H atoms, which carry positive electric charges; subscript "–" refers to points M or N atoms; and N_{tot1} and N_{tot2} are the numbers of positively and negatively charged atoms in the cluster, respectively.

Static dielectric constant ε_0 was calculated via the fluctuations of total dipole moment $\mathbf{d}_{cl}$ [40] as follows:

$$\varepsilon_0 = 1 + \frac{4\pi}{3VkT}\left[\left\langle \mathbf{d}_{cl}^2 \right\rangle - \left\langle \mathbf{d}_{cl} \right\rangle^2\right],$$

where V is the cluster volume and k is Boltzmann's constant.

Dielectric permittivity $\varepsilon(\omega)$ as a function of frequency ω was represented by complex value $\varepsilon(\omega) = \varepsilon'(\omega) - i\varepsilon''(\omega)$, which was determined using the following equation [40, 41]:

$$\frac{\varepsilon(\omega)-1}{\varepsilon_0-1} = -\int_0^\infty \exp(-i\omega t)\frac{dF}{dt}dt =$$

$$= 1 - i\omega\int_0^\infty \exp(-i\omega t)F(t)dt,$$

where $F(t)$ is the normalized autocorrelation function of the total cluster dipole moment,

$$F(t) = \frac{\langle \mathbf{d}_{cl}(t) \cdot \mathbf{d}_{cl}(0) \rangle}{\langle \mathbf{d}_{cl}^2 \rangle}.$$

If the dipole moments of molecules have been determined, the IR absorption cross section is defined as follows [42]:

$$\sigma(\omega) = \left(\frac{2}{\varepsilon_v c \hbar n}\right) \omega \, \mathrm{th}\left(\frac{\hbar\omega}{2kT}\right) \mathrm{Re} \int_0^\infty dt e^{i\omega t} \langle \mathbf{d}_{cl}(t) \cdot \mathbf{d}_{cl}(0) \rangle,$$

where n is the frequency-independent refractive index, ε_v is the dielectric permittivity of vacuum, and c is the speed of light.

Reflection coefficient R is determined as the ratio between the average energy flux reflected from a surface and the incident flux. At the normal incidence of a plane monochromatic wave, the reflection coefficient is determined by the following formula [36]:

$$R = \left| \frac{\sqrt{|\varepsilon_1|} - \sqrt{|\varepsilon_2|}}{\sqrt{|\varepsilon_1|} + \sqrt{|\varepsilon_2|}} \right|^2. \quad (1)$$

Here, it is assumed that the wave incidence occurs from a transparent medium (medium 1) into a medium that may be both transparent and nontransparent, i.e., an absorbing and scattering medium (medium 2). The subscripts at the dielectric permittivity in expression (1) denote the media.

The frequency dispersion of the dielectric permittivity determines the frequency dependence of dielectric loss $P(\omega)$ according to the following expression [37]:

$$P = \frac{\varepsilon'' \langle E^2 \rangle \omega}{4\pi},$$

where $\langle E^2 \rangle$ is the mean-square electric field strength and ω is the frequency of the emitted electromagnetic wave.

Refractive index n and absorption coefficient κ of a medium are determined as follows [36]:

$$n = \sqrt{\frac{\varepsilon' + \sqrt{\varepsilon'^2 + \varepsilon''^2}}{2}}, \quad \kappa = \sqrt{\frac{-\varepsilon' + \sqrt{\varepsilon'^2 + \varepsilon''^2}}{2}}.$$

Coefficient κ determines the rate of wave attenuation during its propagation in a medium.

Total number N_{el} of electrons in cluster unit volume that interact with an external electromagnetic field is defined in the following form [36]:

$$N_{el} = \frac{m}{2\pi^2 e^2} \int_0^\infty \omega \varepsilon''(\omega) d\omega,$$

where e and m are the electron charge and mass, respectively.

Motion at a frequency lower than 1200 cm^{-1} corresponds to librations of molecules, while frequencies higher than 1200 cm^{-1} mainly describe intramolecular vibrations [43], which were realized in the following approximation. Flexible models of molecules were considered. Molecules were provided with flexibility via the procedure that had been developed within the framework of the Hamilton dynamics [44, 45]. Let us consider a diatomic molecule. Assume that atoms a and b in a molecule are separated by a distance of

$$Q = |\mathbf{r}_a - \mathbf{r}_b|,$$

where $\mathbf{r}_a$ and $\mathbf{r}_b$ are the position vectors of the atoms. We denote the corresponding velocities as $\mathbf{v}_a$ and $\mathbf{v}_b$ and express the reduced mass as

$$\mu = \frac{m_a m_b}{m_a + m_b}.$$

The size of the molecule represented by atoms a and b is determined by balancing total potential force $\mathbf{f}(\mathbf{Q}) = -\frac{\partial \mathbf{r}}{\partial \mathbf{Q}} \nabla \Phi(\mathbf{r})$ with centrifugal force $-\mu Q \omega^2$, so that

$$-\mu Q \omega^2 - \mathbf{f}(\mathbf{r}) \frac{\partial \mathbf{r}}{\partial \mathbf{Q}} = 0,$$

where $\omega = |\mathbf{v}_a - \mathbf{v}_b|/Q$ is the angular velocity. Minimizing the contribution of each generalized coordinate to potential energy U, we obtain

$$\frac{\partial}{\partial Q_i} H(\mathbf{r}, \mathbf{v}) = \frac{\partial}{\partial Q_i} \left(\frac{1}{2} \mu_i Q_i^2 \omega_i^2 + U(\mathbf{r}) \right) = 0.$$

This method can be generalized for molecules of any composition [46].

CALCULATION RESULTS

The configuration of a $5NH_3 + (H_2O)_{50}$, system at the 50-ps time moment is illustrated in Fig. 1. It can be seen that, by this time moment, all five ammonia molecules have been absorbed by the water cluster. NH_3 molecules have different orientations; however, as a rule, they tend to be arranged in a manner such that an N atom is hydrogen-bonded with a water molecule. In turn, H atoms of NH_3 molecules "seek" oxygen atoms of water molecules. In a formed $(NH_3)_5(H_2O)_{50}$ cluster, NH_3 molecules remain on the aggregate surface. A newly formed N···H hydrogen bond cannot rupture the network of hydrogen bonds of a dense water core in the cluster center, and the NH_3 molecule cannot penetrate into the aggregate.

The angular distribution (θ-distribution) of the closest geometric neighbors enables us to gain insight into the spatial arrangement of the centers of molecules composing the cluster (Fig. 2). The θ-distribution of a pure water cluster (curve *1*) exhibits three pronounced peaks located at 61°, 96°, and 128°. The

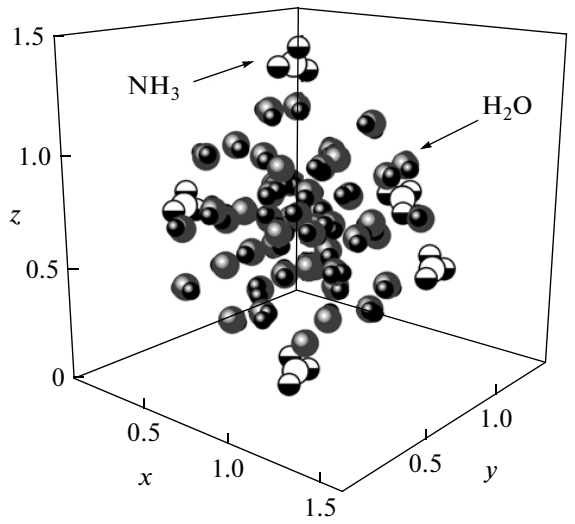

Fig. 1. Configuration of the $(NH_3)_5(H_2O)_{50}$ cluster at the 50-ps time moment.

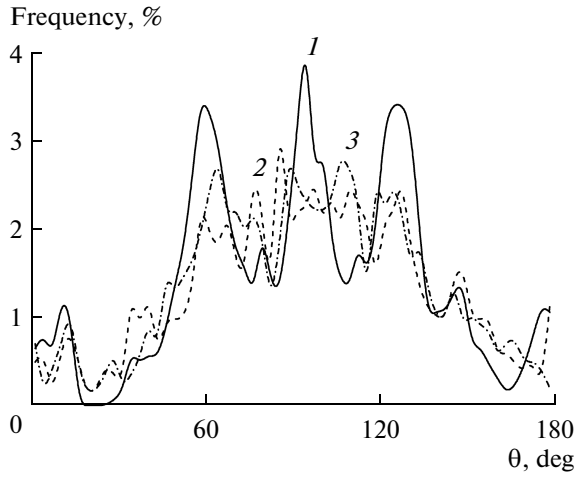

Fig. 2. Angular distributions of closest geometrical neighbors in different clusters: (*1*) $(H_2O)_{50}$, (*2*) $NH_3(H_2O)_{50}$, and (*3*) $(NH_3)_6(H_2O)_{50}$.

fraction of quasi-linear chains composed of three molecules, which are identified with an accuracy of an angle of 15°, in this cluster is 9.2%. The θ-distribution is strongly transformed upon the capture of even one NH_3 molecule (curve *2*); i.e., the pronounced peaks disappear, and the distribution maximum shifts to the position at 87°. The fraction of the quasi-linear chains decreases to 6.6%. After the water cluster adsorbs six ammonia molecules, the middle range of the θ-distribution becomes still more uniform (curve *3*).

In this case, three very intense peaks are located at 66°, 91°, and 109°, while the fraction of the quasi-linear chains is 6.5%.

The size of water clusters affects the real ε' and imaginary ε" components of the dielectric permittivity of the system composed of these aggregates. Figure 3 illustrates the frequency dependences of the complex dielectric permittivity of systems consisting of $(H_2O)_n$, ~~c *n*~~ clusters with $n = 50$ (system I) and 10–50 (system II) and $(NH_3)_{i=1,\ldots,6}(H_2O)_{50}$ clusters (system III). At frequencies $\omega < 3200$ cm^{-1}, the values of ε' and ε" for system I, which is, as a whole, composed of larger clusters, are higher than those for system II. Adsorption of NH_3, molecules by water clusters, i.e., the passage to system III, substantially decreases the ε' and ε" values (curve *3*). On average, in the frequency range of $0 \le \omega \le 3500$ cm^{-1}, the ε' values for system III decreased by factors of 2.7 and 2.1 relative to systems I and II, respectively, while the ε" values diminished 2.2- and 1.8-fold, respectively. The values of ε' and ε" for system III are larger than the corresponding characteristics of bulk water [47, 48] at $\omega > 550$ and 820 cm^{-1}, respectively. The substantial reduction in the ε' and ε" values for the system of clusters containing adsorbed NH_3, molecules is due to the loosening of the structure as a result of the rearrangement of hydrogen bonds.

The IR adsorption spectra calculated for systems I–III, together with the corresponding experimental spectra of liquid water [49] and gaseous ammonia [50], are shown in Fig. 4. Note that, in the frequency range of $0 \le \omega \le 3600$ cm^{-1}, the σ(ω) spectrum of system II is more intense (by a factor of 1.4) than the corresponding spectrum of system I. It is of interest that the IR spectrum intensity for system III is 2.7 times higher than that for system II. This is related to not only the larger sizes of clusters in system III, but also the inhibition of vibrations due to the formation of additional N···H hydrogen bonds. The main peak in the spectrum of system III exhibits a red shift by 610 cm^{-1} relative to the corresponding peak of system II. In turn, the main peak in the IR spectrum of system II is characterized by a blue shift by 70 cm^{-1} with respect to the main peak of bulk liquid water. The second peak in the IR spectrum of system III is located at 1546 cm^{-1}, i.e., close to one of the doubled peaks in the IR spectrum of gaseous NH_3 (1530 cm^{-1}). Another peak of this doublet corresponds to a frequency of 1680 cm^{-1}. In the IR spectrum of system II, the second and other peaks cannot be revealed in the scale of Fig. 4. The added NH_3 molecules enhance the orientational order in the clusters to markedly increase the correlation time of the cluster dipole moments and, as a result, the intensities of the IR absorption spectra.

The integral power $P(\omega)$ of IR radiation emitted by a monodisperse system of water clusters (system I) is 1.3 times higher than that of the system composed of water clusters of nine different sizes (system II) (Fig. 5). System I is characterized by a bimodal $P(\omega)$, spectrum, the main maximum of which corresponds to frequency $\omega = 3340$ cm^{-1}, while system II exhibits

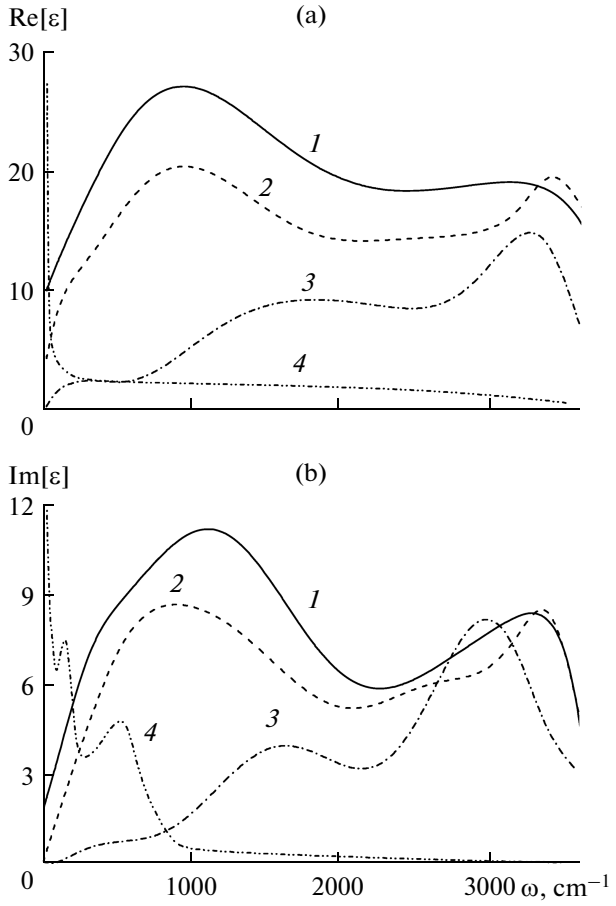

Fig. 3. The (a) real and (b) imaginary components of dielectric permittivity for different cluster systems: (*1*) I, (*2*) II, and (*3*) III. Curves *4* refer to the data of (a) molecular-dynamic calculation [47] and (b) experiment [48].

a unimodal spectrum with the main maximum at $\omega = 3495$ cm^{-1}. A great decrease (by a factor of 10.6) is observed in the intensity of the $P(\omega)$ emission spectrum of system III relative to that of system II. The location of the maximum in the $P(\omega)$ spectrum of system III shifts toward lower frequencies by 830 cm^{-1} relative to the corresponding spectrum of system II. The main emission frequency of system III ($\omega_P = 2667$ cm^{-1}) is lower than the main frequency of absorption ($\omega_\sigma = 2879$ cm^{-1}) by 212 cm^{-1}. This indicates a spontaneous character of IR radiation emission by $(NH_3)_i(H_2O)_{50}$ clusters. An analogous conclusion can be drawn from a comparison of the $\sigma(\omega)$ and $P(\omega)$ spectra for system II, but, in this case, the difference in the main frequencies is not so large (10 cm^{-1}). The weakening of hydrogen bonds in clusters as a result of adsorption of NH_3 molecules drastically reduces the intensity of the cluster emission spectra and, hence, their visibility.

IR reflection spectra $R(\omega)$ of systems I and II are continuous, while that of system III is almost banded

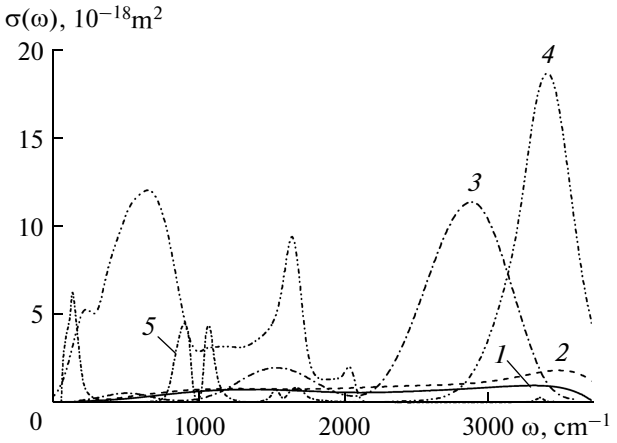

Fig. 4. IR absorption spectra of cluster systems (*1*) I, (*2*) II, and (*3*) III; (*4*) experimental data on $\sigma(\omega)$ for bulk liquid water [49]; and (*5*) experimental spectrum of gaseous NH_3.

(Fig. 6). The average values of reflection coefficient $\bar{R}$ for systems of pure water clusters (systems I and II) are 0.40 and 0.35, respectively, while that of water clusters containing adsorbed ammonia molecules (system III) is 0.20. The substantial reduction in the reflection ability of a system of water clusters after adsorption of NH_3 molecules by the clusters is caused by the formation of a strongly rough surface. Reflected IR radiation maxima of systems I and II correspond to 945 and 1012 cm^{-1}, respectively, while that of system III is observed at 2835 cm^{-1}.

The frequency dependences of absorption coefficients $\kappa(\omega)$ of media and refractive indices $n(\omega)$ are shown for systems I–III in Fig 7. The same figure shows the corresponding experimental spectra of liquid water [51] and a cryogenic NH_3 film [52]. It can be seen that, in the entire frequency range, coefficient κ is higher for systems of pure water clusters than for the $(NH_3)_i(H_2O)_{50}$. system. Coefficient κ determines the rate of wave attenuation in the course of its propagation. Hence, the rate of wave attenuation is higher in systems I and II than in system III at all frequencies under consideration. The frequency-average coefficients κ of systems I and II are 0.81 and 0.72, respectively, while, for system III, it is 0.48. At $\omega > 1100$ cm^{-1}, κ values for cluster systems are always higher than those for liquid water and the cryogenic NH_3. film. Refractive indices n are almost always higher for systems I and II than for system III; i.e., systems I and II have higher optical densities than that of system III. Moreover, the refractive index of system III exhibits a periodic increasing dependence on frequency. At frequenciesω_n index n for cluster systems is higher than for liquid H_2O. The cryogenic NH_3 film exhibits a jump of κ and n in the vicinity of 1058 cm^{-1}.

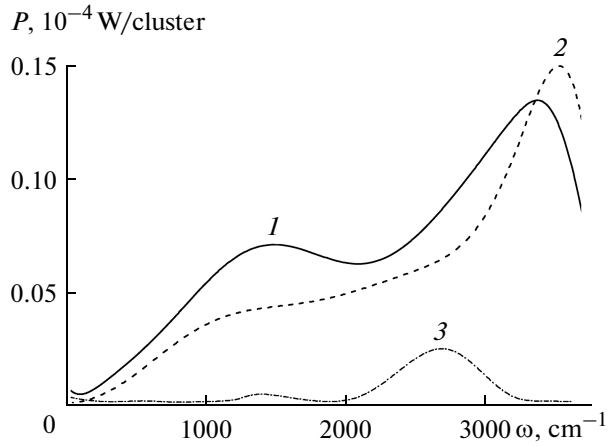

Fig. 5. IR emission spectra for different systems: (*1*) I, (*2*) II, and (*3*) III.

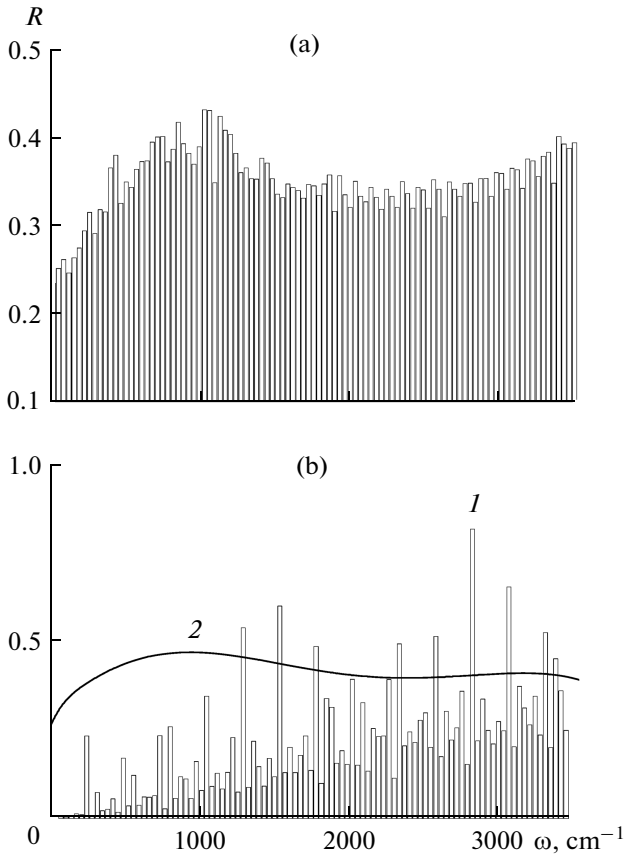

Fig. 6. Coefficients of monochromatic plane electromagnetic wave reflection by different disperse systems: (a) II and (b) (*1*) I and (*2*) III.

For ammonia, not only the boiling and melting temperatures, but also the conductivity and dielectric permittivity, are lower than those for water. Ammonia is easily transformed into a colorless liquid, which strongly refracts light. Hydrogen bonds in liquid ammonia with a density of 0.6814 g/cm³ are much weaker than in water. Ammonia molecule contains only one lone-electron pair in contrast to two pairs in water molecule. This circumstance makes the formation of a branched network of hydrogen bonds between several molecules impossible. Due to the hydrogen bonding, liquid ammonia is, similarly to water, strongly associated and actually nonconducting. Impurities that increase and decrease the number N_{el}, of free electrons are referred to as donors and acceptors, respectively. Upon ionization of an acceptor impurity, electrons are captured from the valence region. Acceptor impurities with ionization energy on the order of thermal energy kT are described by a hydrogen-like model.

The oxidation state of nitrogen atoms is minimum (−3) in ammonia, while, in nitrate radicals, it is maximum (+5). Nitrogen has eight intermediate oxidation states between these extrema. It is of interest to compare (Fig. 8) the dependences of the number N_{el}, of electrons involved in the interaction with electromagnetic radiation on the number i of NH_3 molecules (curve *1*) and nitrate ions (curve *2*) captured by a water cluster. As a whole, the behaviors of the $N_{el}(i)$ dependences upon the adsorption of these two nitrogen-containing components are identical, with the exception of slight differences observed in the range of $1 \le i \le 4$. In both cases, the primary addition of ammonia molecules and NO_3^- ions to a water aggregate causes a strong (by tens of times) reduction in the N_{el} value. The small numbers of electrons that interact with light remain preserved up to the addition of four NH_3 molecules to a water cluster. When the fifth and sixth ammonia molecules are added to the cluster, a tendency toward an increase in N_{el} is observed. However, this increase is insubstantial as compared with the reduction in N_{el} caused by the primary addition of NH_3 molecules to water clusters. As a rule, adsorption of nitrate ions induces larger fluctuations in the number of electromagnetically active electrons than does the adsorption of NH_3 molecules. Upon the adsorption of two, three, five, and six ions, N_{el} increases, while, upon the addition of four ions, it decreases. However, in no case of the presence of NO_3^- ions in the clusters does N_{el} reach the value corresponding to the number of electrons that are active with respect to the radiation in the $(H_2O)_{50}$ cluster. A 2.2-fold larger value of N_{el} ~~i~~ has been obtained for the addition of six NO_3^- ions than for the adsorption of six NH_3 molecules. The complex behavior of the $N_{el}(i)$ function suggests that the electronic structure of the entire cluster is changed as a result of adsorption of each NH_3 molecule (or NO_3^- ion). In other words, the adsorption process appears to be electron-sensitive and essentially nonlinear.

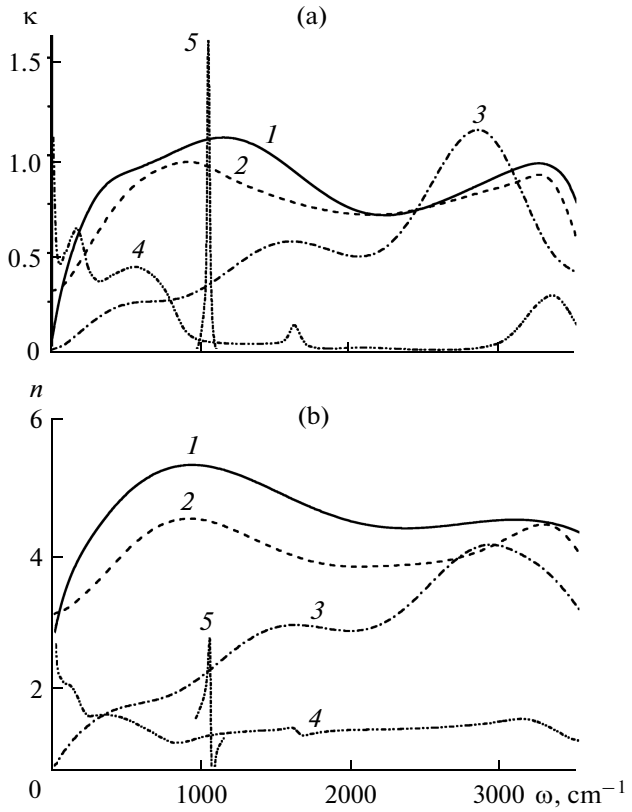

Fig. 7. Frequency dependences of (a) absorption coefficient and (b) refractive index for different systems (*1*) I, (*2*) II, and (*3*) III. Curves *4* and *5* refer to experimental data on (*4*) liquid water [51] and (*5*) cryogenic NH_3 film [52].

CONCLUSIONS

The performed simulation has shown that NH_3 molecules occurring near the surface of a water cluster are absorbed by the latter. As a result, stable $(NH_3)_i(H_2O)_{50}$, clusters containing 1–6 ammonia molecules have been obtained. Due to the internal flexibility of molecules, local structural distortions related to the adsorption of NH_3, molecules by water clusters are minimized. Ammonia molecules are added to the clusters via the formation of new N···H hydrogen bonds. In this case, some O···H bonds may be ruptured and the number of linear chains composed of three atoms decreases by a factor of ≈1.4. The system of water–ammonia clusters exhibits more intense IR absorption spectra and less intense emission and reflection spectra than does the system of pure water clusters. Moreover, after ammonia molecules are adsorbed, the reflection spectrum exchanges its continuous shape for a banded one. The geometrical optics characteristics, i.e., absorption coefficient and refractive index, also decrease throughout the frequency range under examination after adsorption of ammonia molecules by water clusters. Upon the addition of ammonia molecules to water clusters, a noticeable reduction has been observed in the number of electrons that are active with respect to electromagnetic radiation, with subsequent addition of these molecules causing a complex sign-changing variation in the $N_{el}(i)$ function.

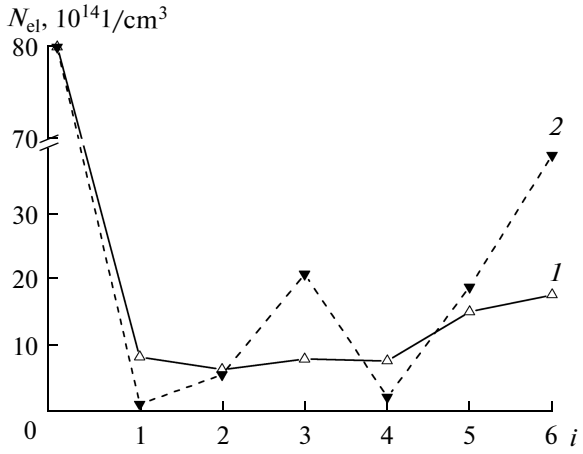

Fig. 8. Densities of electrons interacting with IR radiation for different clusters: (*1*) $(NH_3)_i((H_2O)_{50}$ and (*2*) $(NO_3)_i^-(H_2O)_{50}$,, $i = 1...6$.

REFERENCES

1. Liu, K., Brown, M.G., and Saykally, R.J., *Science* (Washington, D. C.), 1996, vol. 271, p. 62.
2. Buck, U. and Huisken, F., *Chem. Rev.,* 2000, vol. 100, p. 3863.
3. Nauta, K. and Miller, R.E., *Science* (Washington, D.C.), 2000, vol. 287, p. 293.
4. Buck, U., Ettischer, I., Melzer, M., et al., *Phys. Rev. Lett.*, 1998, vol. 80, p. 2578.
5. Sadley, J., Buch, V., Kazimirski, J.K., and Buck, U., *J. Phys. Chem.*, 1999, vol. 103, p. 4933.
6. Mhin, B.J., Kim, J., Lee, S., et al., *J. Chem. Phys.*, 1994, vol. 100, p. 4484.
7. Franken, A., Jalaie, M., and Dykstra, C.E., *Chem. Phys. Lett.*, 1992, vol. 198, p. 59.
8. Schutz, M., Klopper, W., Luthi, H.-P., and Leutwyler, S., *J. Chem. Phys.*, 1995, vol. 103, p. 6114.
9. Fanourgakis, G.S., Apra, E., and Xantheas, S.S., *J. Chem. Phys.*, 2004, vol. 121, p. 2655.
10. Pedulla, J.M., Vila, F., and Jordan, K.D., *J. Chem. Phys.*, 1996, vol. 105, p. 11091.
11. Lee, H.M., Suh, S.B., and Kim, K.S., *J. Chem. Phys.*, 2001, vol. 114, p. 10749.
12. Kryachki, E.S., *Chem. Phys. Lett.*, 1997, vol. 272, p. 132.
13. Lenz, A. and Ojamae, L., *J. Phys. Chem. A*, 2006, vol. 110, p. 13388.
14. Kolaski, M., Lee, H.M., Pak, C., and Kim, K.S., *J. Am. Chem. Soc.*, 2008, vol. 130, p. 103.
15. Lee, H.M., Kim, D., Singh, N.J., et al., *J. Chem. Phys.*, 2007, vol. 127, p. 164311.

16. Stockman, P.A., Burngarner, R.E., Suzuki, S., and Blake, G.A., *J. Chem. Phys.,* 1992, vol. 96, p. 2496.
17. Sadley, J., Moszynski, R., Dobrowolski, C.Cz., and Mazurck, A.P., *J. Phys. Chem. A*, 1999, vol. 103, p. 8528.
18. Donaldson, D.J., *J. Phys. Chem. A*, 1999, vol. 103, p. 62.
19. Lee, C., Fitzgerald, G., Planas, M., and Novoa, J.J., *J. Phys. Chem.*, 1996, vol. 100, p. 7398.
20. Karthikeyan, S., Singh, J.N., and Kim, K.S., *J. Phys. Chem. A*, 2008, vol. 112, p. 6527.
21. Irwin, P.G.J., *Giant Planets of Our Solar System: Atmospheres, Composition, and Structure*, Chichester: Springer-Praxis, 2003.
1 22. Fortes, A.D., Wood, I.G., Vocadlo, L., et al., *J. Appl. Crystallogr.*, 2009, vol. 42, p. 846.
23. Reed, J.W. and Harris, P.M., *J. Chem. Phys.*, 1961, vol. 35, p. 1730.
24. Fortes, A.D., Suard, E., Lemee-Cailleau, M.-H., et al., *J. Am. Chem. Soc.*, 2009, vol. 131, p. 13508.
25. Van Thiel, M., Becker, E.D., and Pimentel, G.C., *J. Chem. Phys.*, 1957, vol. 27, p. 486.
26. Hartmann, M., Miller, R.E., Toennies, J.P., and Vilesov, A., *Phys. Rev. Lett.*, 1995, vol. 75, p. 1566.
27. Dang, L.X. and Chang, T.-M., *J. Chem. Phys.*, 1997, vol. 106, p. 8149.
28. Jorgensen, W.L. and Madura, J.D., *J. Am. Chem. Soc.*, 1983, vol. 105, p. 1407.
29. Benedict, W.S., Gailar, N., and Plyler, E.K., *J. Chem. Phys.*, 1956, vol. 24, p. 1139.
30. Xantheas, S., *J. Chem. Phys.*, 1996, vol. 104, p. 8821.
31. Feller, D. and Dixon, D.A., *J. Phys. Chem.*, 1996, vol. 100, p. 2993.
32. Smith, D.E. and Dang, L.X., *J. Chem. Phys.*, 1994, vol. 100, p. 3757.
33. New, M.H. and Berne, B.J., *J. Am. Chem. Soc.*, 1995, vol. 117, p. 7172.
34. *Spravochnik khimika. T. 1* (Chemist's Handbook), Nikol'skii, B.P., Ed., Leningrad: Khimiya, 1971, vol. 1.
35. Haile, J.M., *Molecular Dynamics Simulation. Elementary Methods*, New York: Wiley, 1992.
36. Landau, L., Lifshitz, E., and Pitaevski. L., *Electrodynamics of Continuous Media*, Oxford: Pergamon, 1984.
37. *Fizicheskaya entsiklopediya. T. 1* (Physical Encyclopedia), Prokhorov, A.M., Ed., Moscow: Sovetskaya Entsiklopediya, 1988, p. 702.
38. Koshlyakov, V.N., *Zadachi dinamiki tverdogo tela i prikladnoi teorii giroskopov* (Problemds of Solid Body Dynamics amd Applied Theory of Gyroscopes), Moscow: Nauka, 1985.
39. Sonnenschein, R., *J. Comput. Phys.,* 1985, vol. 59, p. 347.
40. Bresme, F., *J. Chem. Phys.*, 2001, vol. 115, p. 7564.
41. Neumann, M., *J. Chem. Phys.*, 1985, vol. 82, p. 5663.
42. Bosma, W.B., Fried, L.E., and Mukamel, S., *J. Chem. Phys.*, 1993, vol. 98, p. 4413.
43. Stern, H.A. and Berne, B.J., *J. Chem. Phys.*, 2001, vol. 115, p. 7622.
44. Lemberg, H.L. and Stillinger, F.H., *J. Chem. Phys.*, 1975, vol. 62, p. 1677.
45. Rahman, A., Stillinger, F.H., and Lemberg, H.L., *J. Chem. Phys.*, 1975, vol. 63, p. 5223.
46. Saint-Martin, H., Hess, B., and Berendsen, H.J.C., *J. Chem. Phys.*, 2004, vol. 120, p. 11133.
47. Neumann, M., *J. Chem. Phys.*, 1986, vol. 85, p. 1567.
48. Angell, C.A. and Rodgers, V., *J. Chem. Phys.*, 1984, vol. 80, p. 6245.
49. Goggin, P.L. and Carr, C., in *Water and Aqueous Solutions,* Neilson, G.W. and Enderby, J.E, Eds., Bristol: Adam Hilger, 1986, vol. 37, p. 149.
50. Kleiner, L., Brown, R., Tarrago, G., Kou, Q.-L., et al., *J. Mol. Spectrosc.*, 1999, vol. 196, p. 46.
51. Downing, H.D. and Williams, D., *J. Geophys. Res.*, 1975, vol. 80, p. 1656.
52. Wood, B.E. and Roux, J.A., *J. Opt. Soc. Am.*, 1982, vol. 72, p. 720.

SPELL: 1. Appl